

TITLE PAGE

Latonduine analogues restore F508del-CFTR trafficking through the modulation of PARP-3 and PARP-16 activity.

Graeme W. Carlile, Renaud Robert, Elizabeth Matthes, Qi Yang, Roberto Solari, Richard Hatley, Colin M. Edge, John W. Hanrahan, Raymond Andersen, David Y. Thomas and Véronique Birault

Dept. of Biochemistry McGill University Montréal Québec Canada, H3G1Y6

GWC, QY, DYT

Cystic Fibrosis Translational Research Center, McGill University Montréal Québec Canada, H3G1Y6

GWC, RR, EM, Q Y, JWH, DYT

Dept. of Physiology McGill University Montréal Québec Canada, H3G1Y6

RR, EM, JWH

GSK Respiratory Therapeutic Area Unit, GlaxoSmithKline Medicines Research Centre, Gunnels Wood Road, Stevenage, Hertfordshire SG1 2NY, United Kingdom

RS, RH, VB

R&D Platform Technology & Science, GlaxoSmithKline Medicines Research Centre, Gunnels Wood Road, Stevenage, Hertfordshire SG1 2NY, United Kingdom

CME

Departments of Chemistry and Earth, Ocean & Atmospheric Sciences, University of British Columbia, Vancouver, British Columbia, Canada V6T1Z1

RA

Faculty of Medicine National Heart and Lung Institute, Imperial College London, South Kensington Campus, London SW7 2AZ United Kingdom

RS

The Francis Crick Institute 215 Euston Road, London NW1 1HG United Kingdom

VB

RUNNING TITLE PAGE

Running title

Latonduine rescues F508del-CFTR by PARP-3 inhibition and UPR modulation by PARP-16

Correspondence

Dr. Graeme W. Carlile
Department of Biochemistry/ Cystic Fibrosis Translational Research Center
McGill University
3655 Promenade Sir William Osler Room 900
Montréal Québec Canada, H3G1Y6

E-mail: graeme.carlile@McGill.ca

Abstract 237 words

Introduction 562 words

Discussion 1426 words

Text pages 43 (including figure legends)

Figures 6

Supplementary Figures 9

Supplementary Table 1

References 34

MOL #102418

ABBREVIATIONS

UPR; unfolded protein response

IRE-1; inositol-requiring enzyme 1

CFTR cystic fibrosis transmembrane conductance regulator

PARP poly ADP ribose polymerase

HEPES 4-(2-hydroxyethyl)-1-piperazineethanesulfonic acid

HEK cells; human embryonic kidney cells

BHK cells; baby hamster kidney cells

CFBE cells; cystic fibrosis bronchial epithelial cells

ABSTRACT

Cystic Fibrosis (CF) is a major lethal genetic disease caused by mutations in the CF transmembrane conductance regulator gene (CFTR). This encodes a chloride ion channel on the apical surface of epithelial cells. The most common mutation in CFTR (F508del-CFTR) generates a protein that is misfolded and retained in the endoplasmic reticulum. Identifying small molecules that correct this CFTR trafficking defect is a promising approach in CF therapy. To date however only modest efficacy has been reported for correctors in clinical trials. We identified the marine sponge metabolite latonduine, as a corrector. We have now developed a series of latonduine derivatives that are more potent F508del-CFTR correctors with one (MCG315) having 10 fold increased corrector activity and an EC₅₀ of 72.25nM. We show that the latonduine analogues inhibit poly-ADP ribose polymerase (PARP) isozymes 1, 3 and 16. Further our molecular modeling studies point to the latonduine analogues binding to the PARP nicotinamide-binding domain. We established the relationship between the ability of the latonduine analogues to inhibit PARP 16 and their ability to correct F508del-CFTR trafficking. We show that latonduine can inhibit both PARP-3 & 16 and that this is necessary for CFTR correction. We demonstrate that latonduine triggers correction by regulating the unfolded protein response (UPR) activator, inositol-requiring enzyme (IRE-1) activity via modulation of the level of its ribosylation by PARP-16. These results establish latonduines novel site of action as well as its proteostatic mechanism of action.

INTRODUCTION

Cystic fibrosis (CF) is a common lethal genetic disease caused by mutations in the gene encoding the cystic fibrosis transmembrane conductance regulator (CFTR), a cAMP-activated anion channel normally expressed at the apical membrane of secretory epithelial cells (Riordan et al., 1989). An in-frame deletion of a triplet encoding phenylalanine at position 508 (F508del-CFTR) is the most common mutation and is found on at least one chromosome in approximately 90% of patients (Cheng et al., 1990). This mutation prevents correct folding and trafficking of the mutant channel to the plasma membrane. When F508del-CFTR surface expression is restored, it retains some function however its stability in the plasma membrane and open probability are reduced compared with wild-type channels (Hwang and Sheppard, 2009; Lukacs et al., 1993).

The ability of some small molecules to partially restore F508del-CFTR trafficking has encouraged the development of drug candidates (Carlile et al., 2007; Clancy et al., 2012; Egan et al., 2004; Robert et al., 2010; Robert et al., 2008; Rubenstein et al., 1997; Sato et al., 1996; Van Goor et al., 2011). However, only VX-809 (Lumacaftor) and its analogue VX-661 have progressed to clinical trials (Clancy et al., 2012) with VX-809 having only limited success in restoring F508-del-CFTR function in patients (Grasemann et al 2010). Despite this VX-809 in combination with ivacaftor (ORKAMBI) has recently been approved by the U.S. Food and Drug Administration (FDA) for people with CF ages 12 and older who are homozygous for the F508del mutation (www.vrtx.com). We reasoned that the small number of lead compounds identified to date may be at least in part due to the limited amount of chemical space encompassed by available compound libraries. To address this we previously screened a library of marine sponge extracts and

identified the latonduine compound family (Carlile et al., 2012). Latonduine is a corrector of F508del-CFTR whose correction activity is dependent on its inhibition of members of the poly (ADP-ribose) polymerase (PARP) family.

In the present work we have synthesized latonduine analogues and evaluated their ability to correct F508del-CFTR trafficking. One analogue MCG315 gave a response 10-fold greater than latonduine itself.

The analogues were then used to examine the dependence of F508del-CFTR trafficking correction on the inhibition of PARPs 1, 3 and 16. It was found that concerted inhibition of PARPs-3 and 16 together triggered correction. It was decided to focus on PARP-16 as recent reports have found (Jwa and Chang, 2012) that it is a tail anchored protein located at the endoplasmic reticulum membrane and that it may regulate the unfolded protein response (UPR) through the ribosylation of IRE-1 a key sensor that activates the UPR. A strong positive correlation was found between the inhibition of PARP-16 by different analogues and the extent of F508del-CFTR correction. We also show using a biotinylated version of latonduine that latonduine can bind directly to purified recombinant PARP-16.

Latonduine can block the ribosylation of IRE-1 by PARP-16 to and also block the ribosylation mediated increase of both kinase and RNAase activity. This suggests that latonduine mediated F508del-CFTR correction is by preventing the activation of the UPR by IRE-1 through inhibition of PARP-16 mediated ribosylation that causes IRE-1 activation. However, experiments with IRE-1 inhibitors and siRNA to IRE-1 demonstrate that some IRE-1 activity is necessary for correction. This maintenance of a certain level

MOL #102418

of IRE-1 activity is clearly critical to the proteostatic equilibrium necessary for latonduine mediated F508del-CFTR correction.

MATERIALS AND METHODS

HTS Protocol

The screen assay was performed as described previously (Carlile et al., 2007). Briefly, BHK cells stably expressing F508del-CFTR bearing three tandem haemagglutinin-epitope tags (3HA) in the fourth extra-cellular loop were plated in 96 well plates and treated with compounds. Latonduine analogues were tested initially at 10 μ M for 24 hours, and then cells were fixed with 4% paraformaldehyde and immunostained. Surface CFTR was measured using a mouse monoclonal anti-HA antibody (Sigma Aldrich USA, Cat. H9658). Hits were defined as compounds that consistently gave signals that were three standard deviations above untreated control cells and were not intrinsically fluorescent. A similar protocol was utilized to monitor the surface expression of endogenous CD44. In this case the primary antibody used was an anti-CD44 mouse monoclonal antibody (a kind gift of Prof. Katherine Borden, IRIC University of Montreal).

Immunoblotting

CFTR expression in CFBE41o- cell lysates was assessed by immunoblotting as described previously (Carlile et al., 2012). Western blots were probed with the monoclonal anti-CFTR antibody 24-1 (R&D Systems USA. Cat. MAB25031). The relative amount of each CFTR glycoform was estimated by densitometry using the ImageJ program (Rasband, 2011).

Latonduine pulldown studies

Biotinylated latonduine pulldown

The latonduine pulldown was performed as before (Carlile et al., 2012). Briefly, human recombinant PARP-16 (the construct was a kind gift of Prof. Herwig Schuler, Karolinska Institute) was diluted in buffer B (25mM HEPES, pH 7.5 115mM potassium acetate, 2.5mM magnesium chloride, protease inhibitors (Roche)) and adjusted to 10ng/ml with buffer B. The protein sample was pre-cleared by incubation at 4⁰C with beads (DynaL streptavidin M-280) that had previously been incubated in 1 mM biotin for 1h and then removed. Biotin labeled latonduine A (5pmol) and beads (DynaL streptavidin M-280) were added and incubated for 3h at 4⁰C. The beads were then collected using a magnetic tube rack and the supernatant was removed by washing 3 times with buffer B (with 0.2% Triton X-100). The samples were then resolved by SDS-PAGE and visualized using Coomassie blue stain.

PARP enzymatic assays

A selection of PARP enzymes was used in these studies: PARP-1 (Enzo life sciences 201-063-C020), PARP-2 (Enzo life sciences 201-064-C020), PARP-3 (Enzo life sciences 201-170-C020), PARP-4 (Enzo life sciences 201-286-C010), PARP-5a (BPS Bioscience 80504), PARP-5b (BPS-bioscience 80505), PARP-11 (BPS Bioscience 80511) and PARP-16 (the construct was a kind gift of Prof. Herwig Schuler, Karolinska Institute). The HT Universal Chemiluminescent PARP Assay Kit with histone coated Strip Wells

MOL #102418

(Trevigen, Gaithersburg, MD, Cat. 4685-096-K) was used to test PARP inhibition by latonduine as per the manufacturer's instructions. PARP inhibitors PJ34 and ABT888 were obtained from SelleckChem (Cat. S7300 and S1004 respectively).

For testing of PARP-16 a modified version of the assay was undertaken. Recombinant human full length IRE-1 tagged with a 6xHIS tag was used as a substrate all other PARPs tested used anchored-histone proteins provided in the Kit. The manufacturers protocol was used except that a 1.5ml tube was used and not the 96 well plate provided. After the IRE-1 was incubated with the enzyme and reagents Nickel-agarose beads (10 μ l) per reaction were added and incubated for 1 hour. The rest of the protocol was performed on the IRE-1 bound to the beads. In the final step the IRE-1 bound beads were transferred to a 96 well dish and exposed to the two necessary chemiluminescent reagents for the reaction to occur.

High Throughput siRNA assay

SiRNA knock down: HEK293 expressing F508del-CFTR-3HA or wild-type CFTR-3HA were used. PARP-16 specific or non-targeting (NT) siRNAs were arrayed into a 96-well plate and used for transduction as described in the manufacturer's instructions. HEK CFTR WT cells were added to the plate as controls. Next day the medium was exchanged for fresh medium containing antibiotics and MCG315 or DMSO. Surface expression was analyzed 24 h later as described previously (Carlile et al., 2012).

Voltage-clamp studies of CFBE41o- cell monolayers

Short-circuit current (I_{sc}) was measured across monolayers mounted in modified Ussing

MOL #102418

chambers (EasyMount, Physiologic Instruments, San Diego CA) and voltage clamped using a VCCMC6 multichannel current-voltage clamp (Physiologic Instruments). The CFBE cell line used is the CFBE41o⁻ derived from a CF patients bronchial epithelial cells and stably infected withTranzVector lentivectors containing either wt or F508del-CFTR.

They were kindly provided by J.P. Clancy (University of Alabama)(Bebok Z, 2005) . CFBE41o⁻ cells (10⁶) were seeded onto 12-mm fibronectin-coated Snapwell inserts (Corning Inc., Tewksbury MA) and the apical medium was removed after 24h to establish an air-liquid interface. Trans-epithelial resistance was monitored using an EVOM epithelial volt-ohmmeter, and monolayers were used when the resistance was 300-400 Ω .cm². CFBE41o⁻ monolayers expressing F508del-CFTR were treated on both sides with optiMEM containing 2% (v/v) FBS and either 0.1% DMSO (negative control) or 10 μ M test compound. Some cells were incubated at 29°C for 24h as a positive control before being mounted. Apical membrane Cl⁻ conductance was isolated functionally by permeabilizing the basolateral membrane with 200 μ g/ml nystatin and imposing an apical-to-basolateral Cl⁻ gradient. The basolateral bathing solution contained (in mM) 1.2 NaCl, 115 Na-gluconate, 25 NaHCO₃, 1.2 MgCl₂, 4 CaCl₂, 2.4, KH₂PO₄, 1.24 K₂HPO₄ and 10 glucose (pH 7.4). CaCl₂ concentration was increased to 4mM to compensate for the chelation of calcium by gluconate. The apical solution contained (in mM) 115 NaCl, 25 NaHCO₃, 1.2 MgCl₂, 1.2 CaCl₂, 2.4 KH₂PO₄, 1.24 K₂HPO₄ and 10 mannitol (pH 7.4). Mannitol was used instead of glucose to eliminate currents mediated by Na⁺-glucose co-transporters. Successful permeabilization of the basolateral membrane was obvious from the reversal of I_{sc} under these conditions. Solutions were continuously gassed and stirred

MOL #102418

with 95% O₂-5% CO₂ and maintained at 37°C. Ag/AgCl reference electrodes were used to measure trans-epithelial voltage and pass current. Pulses (1mV amplitude, 1s duration) were delivered every 90s to monitor resistance. The voltage clamps were connected to a PowerLab/8SP interface for data collection. CFTR was activated by adding 10μM forskolin + 50μM genistein to the apical bathing solution. This was sensitive to the CFTR channel blocker CFTR_{inh}-172 (10μM(Ma et al., 2002)), confirming that the conductance mediated by F508del-CFTR channels

Molecular modeling

Crystal structures of the three of the PARP family members used in the modeling study (PARP-1: 1A26; PARP-3: 3C4H and PARP-16: 4F0D) were from the Protein Data Bank (Berman et al., 2000). The only PARP-1 structure available is from chicken homolog rather than human, however, all residues in the putative binding site appear conserved except Q763, which is a glutamate in the human isoform, are conserved.

Models of latonduine A, MCG171, MCG172, MCG240, MCG315 and MCG559 were generated using the Molecular operating environment (MOE, 2012) program. Molecules were docked into each of the three enzymes studied by defining elastic restraints based on observed distances between the amide of DR231 and PARP-3 in the 3C4H crystal structure. The enzyme was fixed *in situ*, using the Potential Fix command, and any ligand clashes were ameliorated using low mode molecular dynamics or stochastic searching within the MOE conformational analysis utility. In all cases plausible binding

modes resulted, although there were discernible differences in orientation and likely interactions with the enzymes.

IRE-1 enzymatic assays

Kinase assay: the ADP-Glo™ Kinase Assay Kit, (V9101, Promega) was used to test IRE-1 kinase activity as per the manufacturer's instructions. Recombinant human IRE-1 α was utilized in the experiments at a final concentration of 200nM in 20 μ l. Luminescence was measured using a PheraStar (BMG Labtech).

RNase Assay: the Xbp1 splicing assay (Xbp1 BHQPlus Probe, Biosearch Technologies) was carried in a 96 well plate format. Briefly, 0.5 μ l of the compound of interest was added to 24.5 μ l of RNase buffer (20mM Hepes, pH7.4, 1mM Magnesium Acetate, Potassium Acetate) containing 200nM human IRE-1 α . This solution was then mixed with 25 μ l of substrate buffer containing 1 μ M XBP1 probe, 2mM ADP and 1mM DTT. Fluorescence was read immediately at 612 and 670nm (Synergy; Biotech Instruments).

Chemistry section

Latonduine synthesis has been previously described (Carlile et al. 2012, Linington et al 2003). Of the seven analogues the synthesis of 2: MCG315 (2,3-dihydro-1H-2-benzazepin-1-one) (Corriu et al. 1993) and MCG980 (2,3-dibromo-1H-pyrrolo[2,3-c]pyridin-7(6H)-one) (Sosa et al. 2000) have been previously described. A third analogue MCG559 (2,3-dimethyl-6,7-dihydropyrrolo[2,3c]azepin-8(1H)-one) is commercially available (CAS Registry Number 1392102-10-1). The protocols for the

synthesis of the other latonduine analogues discussed in this paper are found in the supplementary methods section.

Statistical Analysis

Statistical analyses were performed using GraphPad Prism 6 (GraphPad Software, La Jolla, CA) including linear regression and curve fitting to obtain EC₅₀s. Data were expressed in graphs as means with error bars showing S.D. Composite concentration response data were fitted to the Hill equation:

$$Y = \text{Bottom} + (\text{Top} - \text{Bottom}) / (1 + 10^{((\text{LogEC}_{50} - X) * \text{HillSlope})})$$

Y is the percentage increase in cell surface CFTR signal, X is the concentration of compound necessary to achieve this response and EC₅₀ is the compound concentration that produces half-maximum compound response were used to calculate the mean and S.E.M. For graphical presentation, data sets from individual experiments were normalized to the maximum compound response in the experiment, making it possible to calculate the mean and the S.E.M. for each data point. The averaged data points were then fitted to the Hill equation and plotted together with the resulting curve.

Levels of significance were established with a P value * = 0.1, ** a value of, 0.05 and *** a value of 0.005 were predetermined as statistically significant levels of difference (see figure 5). Significance was determined using one and two-way t-tests. All experiments were successfully performed on at least three separate occasions and all samples were prepared for each experiment in triplicates.

RESULTS

Latonduine analogues

Three features of latonduine structure were examined. The effects of removing of the aminopyrimidine ring and modifying substituents on the pyrrole ring (MCG980, MCG559; MCG172, MCG170) (Fig. 1A). In particular we substituted the bromine atom with methyl substituents to generate compounds MCG172 and MCG559. We then explored changes to the substituted pyrrole ring for a phenyl ring, (MCG315). Finally we examined the azepin ring by synthesizing the analogues MCG171 and MCG240.

Latonduine analogues correct the trafficking of F508del-CFTR

To determine if any of the latonduine modifications generated were able to correct F508del-CFTR we tested them using a cell-based HTS assay. We found that all the analogues of latonduine trigger some level of F508del-CFTR correction, with four compounds giving a >20% percent increase in the cell surface CFTR signal (MCG172, MCG240, MCG315 and MCG559). MCG315 gave the strongest response (35% of wild type surface expression signal; Fig. 1B); it had little effect on wild-type CFTR expression, and also no significant response in parental BHK cells (Supplemental. Fig. 1).

Latonduine analogues increase the levels of the mature glycoform of F508del-CFTR

CFTR protein maturation can be used as a marker of CFTR trafficking, upon protein translation CFTR becomes immaturely glycosylated in the ER and appears as a discrete band on an immunoblot known as band B. In due course if the CFTR protein is then trafficked to the Golgi apparatus its glycosylation state is altered and a band with a

larger apparent molecular weight, band C will be seen. Hence the trafficking of CFTR from the ER to the Golgi can be monitored. CFTR protein maturation upon latonduine and latonduine analogue treatment was determined by immunoblotting. Maturation was indicated by the appearance of the mature glycosylated (band C) form of CFTR in BHK cells after 1 μ M latonduine or latonduine analogue (24h). Treatment with latonduine and some analogues (MCG172, MCG240, MCG315, MCG559) partially corrected F508del-CFTR processing as shown by increased band C (Fig. 1C). Thus the analogues that gave the strongest signal in the HTS assay (>20% increase in surface CFTR; Fig. 1B) also generated increased band C in cells expressing F508del-CFTR. Quantification of the CFTR signal using Image J revealed that ~40% of the F508del-CFTR was complex glycosylated after treatment with MCG172 or MCG315 (Fig. 1D). Thus, latonduine and these four analogues (MCG172, MCG240, MCG315 and MCG559) cause significant rescue of F508del-CFTR trafficking in BHK cells.

Latonduine analogues correct F508del-CFTR function

To determine if the F508del-CFTR corrected by latonduine and its analogues is functional, polarized CFBE41o⁻ monolayers were exposed to each compound (10 μ M for 24 h) then tested for CFTR function by monitoring the forskolin-stimulated short circuit current (I_{sc}) in Ussing chambers. Latonduine and four of its analogues (MCG172, MCG240, MCG315, MCG559) gave positive responses in Ussing chambers (Fig.2). The same four analogues that increased apical Cl⁻ conductance indicative of functional CFTR in the apical membrane of the polarized cells also triggered the appearance of band C in immunoblots of BHK cell lysates (Fig. 1C). Of these MCG315 gave functional rescue

equivalent to ~3.2% of the wild-type CFTR current. This represents a 9.85-fold increase in functional correction by MCG315 compared to latonduine and ~30% of the response after treatment with VX-809 in the same assay (Figs. 2A, 2B). Thus latonduine analogues cause a significant correction of F508del-CFTR activity in polarized CFBE airway epithelial cell monolayers.

Dynamics of MCG315 correction in comparison to Latonduine

MCG315 is the most potent corrector of the latonduine analogue series. To quantify its potency we determined the EC₅₀ for correction of CFTR and compared it with latonduine. MCG315 and latonduine were tested over a range of concentrations using the HTS assay (Fig. 2C). Both compounds yielded a similar correction profile, with detectable signal appearing at 10nM and peaking at 10μM. Latonduine and its analogues had little effect on wild-type CFTR trafficking at all concentrations tested (Supplemental. Fig. 1). This experiment indicates the EC₅₀ for latonduine is 62.14nM and for MCG315 is 72.25nM.

It has previously been noted that there was a decrease in response for latonduine at 100μM (Carlile et al. 2012). To determine if latonduine family members triggered this drop in response by cellular toxicity at higher concentrations the effect of MCG315 was tested using dye exclusion (Supplemental. Fig. 2). The results show that indeed at 100μM and to a lesser extent at 10 μM levels of cell death are significantly elevated.

To estimate the rates of correction by latonduine and MCG315 we measured the time course of the appearance of F508del-CFTR at the cell surface appearance using the HTS assay (Fig. 2D). Neither compound induced significant correction of F508del-CFTR within 4h of treatment and only attained significant levels of correction after 18 h. Correction reached a maximum after 48 h of latonduine treatment as reported previously

(Carlile et al., 2012), whereas MCG315 gave maximal correction within 24 h. The maximal CFTR signal detected at the cell surface was similar for both compounds and persisted for more than 72 hours, thus both compounds increased surface CFTR expression >60 hours.

Poly-ADP ribose polymerases are targets of latonduine analogues

Our previous work showed that latonduine binds to PARP family members especially PARP-3, and triggers CFTR correction by inhibiting their enzymatic activity (Carlile et al., 2012). Intriguingly, recent research has highlighted a possible role for PARP-16, in ER protein folding regulation (Jwa and Chang, 2012). To determine if latonduine can interact directly with PARP-16 we undertook pulldown studies with recombinant PARP-16 and confirmed that biotinylated latonduine can bind PARP-16 directly (Fig. 3A, 3B) and that this binding can be competed away by both increasing amounts of latonduine and separately MCG315 (Carlile et al 2012).

To establish the ability of the latonduine analogues to inhibit members of the PARP family they were tested in assays that measure the activity of PARPs 1, 3 and 16 (Fig. 3C). It should be noted that VX-809 and ABT888 were used as controls. ABT888 is a PARP-1 inhibitor, and VX-809 is a strong CFTR corrector with no reported ability to inhibit any PARP family enzymes (Anjos et al., 2012; Van Goor et al., 2011). Against PARP-1 the analogues of latonduine gave varying degrees of enzyme inhibition, with 6 of the seven analogues causing $\geq 50\%$ inhibition, including all four of the analogues yielding a positive response in Ussing chambers. However MCG559 a compound that

gave the weakest positive using chamber response for a corrector (Fig 2A) nevertheless caused the strongest inhibition of PARP-1 of any analogue including MCG172 MCG240 or MCG315. In contrast to PARP-1, the sensitivity of PARP-3 to inhibition by latonduine analogues paralleled their relative abilities to rescue F508del-CFTR function with the four most potent correctors reducing PARP-3 activity by $\geq 60\%$. However, this correlation was not always observed for example the strongest PARP-3 inhibitor was MCG240 (94% reduction) whereas MCG315 gave the most correction. PARP-16 was also sensitive to Latonduine analogues however in contrast to PARP-3 there was a strong direct correlation for every analogue between the levels of PARP-16 inhibition and F508del-CFTR trafficking correction.

It should be noted that the VX-809 did not inhibit any of the three PARPs tested and ABT888 was the strongest PARP-1 inhibitor tested but was not able to inhibit either PARPs-3 or 16.

MCG315 gave the greatest correction of F508del-CFTR in Ussing chambers and also the highest level of PARP-16 inhibition (97% inhibition). To determine the effectiveness of MCG315 as a PARP-16 inhibitor, assays were performed over a range of concentrations (Supplemental. Fig. 4), which yielded an EC_{50} of 2.4 nM.

This raised the question as to whether MCG315 was a general PARP inhibitor or more specific for PARP-3 and 16. To answer this MCG315 was tested for its ability to inhibit a panel of PARPs (PARPs 1, 2, 3, 4, 5a, 5b, 11 and 16)(Fig. 3D and Supplemental. Fig. 3&4). The results show that MCG315 is a potent inhibitor of PARPs 3 and 16 and to a lesser extent PARP 1 (IC_{50} s of 3.7nM for PARP-3, 2.4nM for PARP-16 and 17.0 μ M

for PARP-1). MCG315 by contrast is a weak inhibitor of PARPs 2, 4, 5a, 5b and 11 with IC_{50} s at $1\mu\text{M}$ and above (Supplemental. Fig 4 and Supplemental. Table 1).

Molecular modeling of PARPs 1, 3 and 16

To rationalize the observed inhibition of PARP-16 relative to PARP-1 and PARP-3 we undertook an analysis of the structural differences between PARPs 1, 3 and 16. All three x-ray diffraction structures contain a similarly shaped nicotinamide binding pocket for NAD^+ , with amide recognition provided by a conserved glycine in a strand of beta-sheet (Fig. 4A, 4E). In the PARP-16 structure this glycine (G153) provides hydrogen bonds from both its amide NH and carbonyl C=O to the amide of the NAD^+ mimetic (Fig. 4A, 4B). PARP-1, and PARP-3 also have a likely hydrogen bond from a neighboring serine hydroxyl to the carbonyl oxygen of an amide or lactam. Indeed this serine (S422) in PARP-3 makes a hydrogen bond to the carbonyl of the inhibitor DR2313, a tetrahydrothiopyranpyridinone. The rest of the amide recognition consists of a wall provided by the conserved histidine and tyrosine aromatic side chains from the so-called HYE motif and a wall formed by a conserved tyrosine on the opposite face. These form a narrow cleft with the amide recognition element at the bottom, (Fig. 4A, 4E).

One difference is in the alpha-helical regulatory domains. The PARP-16 N-terminal domain is remote from the NAD^+ pocket whereas the long α -helix in PARP-1 and PARP-3 forms part of the pocket, which is absent in PARP-16. (Fig.4C). Another difference is the ADP binding site, which seems half-formed in the PARP-16 structure. This is due to residues V223-P250 being disordered in the crystal and the lack of coordinates for an area roughly corresponding to residues S947-N987 in PARP-1.

Molecular Modeling of Latonduine and analogues onto PARPs

All latonduine analogues contain a lactam functional group that could potentially mimic the amide of nicotinamide. Our hypothesis was that these molecules bind in the nicotinamide binding pocket in competition with NAD⁺, as this is a known mechanism of PARP inhibitors (DR2313) (Lehtio et al 2009). Previously we showed that latonduine binds directly to the catalytic domain including the NAD pocket of PARP-1 (Carlile et al., 2012).

The molecules built using MOE-2012 (latonduine, MCG171, MCG172, MCG240, MCG315 and MCG559) were docked into each of the three enzymes studied by defining elastic restraints based on the distances observed between the amide of DR2313 and PARP-3 in the 3C4H crystal structure (Mhlanga et al., 2013). Plausible binding modes were obtained in all cases, although there were differences in orientation and likely PARP interactions.

Latonduine has an extra, fused aminopyrimidine ring when compared with most of the analogues, which are pyrroloazepinones. Aspartate284 of PARP-3, which is on the long α -helix mentioned previously, may form a salt bridge with the basic amine of this ring. The amine also points towards the D-loop, a region of the enzyme that has been shown to be somewhat mobile (Lehtio et al., 2009). In PARP-3, this loop contains Glycine406, which may move by about 1 Å to accommodate the potent ligands. In the latonduine docking model the carbonyl group is available to form a hydrogen bond with the amine (Fig. 4D). These extra interactions may explain the better inhibition of PARP-3 compared to PARP-1.

The smallest analogue is MCG315, a dihydrobenzoazepinone. This has a larger benzo rather than pyrrolo group fused to the azepinone ring, but no substituents in the 7- or 8-positions. This molecule has affinity for PARP-1 and PARP-3 but is the most potent inhibitor of PARP-16. This may be due to interactions with the wall at the end of the nicotinamide pocket adjacent to the ADP binding site. This is composed of a salt bridge between lysine and glutamate in both PARP-1 and PARP-3, against which the 7- and 8-benzo hydrogens pack. In PARP-16, the wall is made of leucine and tyrosine; this slightly larger pocket allows MCG315 to fit deeper in (Fig. 4).

The same wall appears crucial in determining the fit of the analogues, as their inhibition of the enzymes relates to the size of the 2- and 3-substituents on the pyrrole ring. For instance, MCG559 has a methyl at both positions and is more potent than MCG172, which has a larger 2-bromo substituent. Similarly, MCG240 is a more potent inhibitor across all three enzymes than its isomer MCG171, suggesting the 3-bromo cannot be accommodated as easily as 3-methyl. Thus the modeling studies suggest that latonduine and its analogues inhibit members of the PARP family by binding into the nicotinamide pocket and that the differences in inhibitory effect relate to their ability to bind in this pocket.

SiRNA knockdown of PARP-16 expression reduces the amount of MCG315 needed for maximum rescue of F508del-CFTR.

We have previously demonstrated that latonduine works through PARP-3 to trigger F508del-CFTR correction (Carlile et al 2012). Here, we decided to discover what role PARP-16 played in latonduine family CFTR correction. To determine if correction

by MCG315 depends on PARP-16 inhibition we used siRNA to PARP-16 and PARP-3 separately and together to knockdown expression and tested whether less MCG315 was required for CFTR correction (Fig. 4F). HEK293 cells expressing F508del-CFTR-3HA were used for these experiments due to the greater availability of siRNAs for human genes. Cells were transfected with siRNA targeting the PARPs mRNA transcripts, and cultured for 24h, treated with a range of MCG315 concentrations for an additional 24h, then assayed for F508del-CFTR trafficking to the cell surface. SiRNA reduced PARP-16 and PARP-3 expression by $\geq 80\%$ (Supplemental. Fig. 5A). As previously reported reduction in amount of PARP-3 reduced the amount of MCG315 necessary for CFTR correction with the EC_{50} for MCG315 going from 72nM to 3.5nM. The PARP-16 knockdown also reduced the EC_{50} for correction by MCG315 from 90nM to 5nM, suggesting that MCG315 also rescues F508del-CFTR by inhibiting PARP-16. Interestingly when one uses siRNA to both PARPs-3 & 16 the level of surface F508del-CFTR is elevated even in the absence of MCG315 and although the level of correction does increase with the addition of MCG315 it does not surpass the level of correction attained by MCG315 on its own. Hence the results suggest that latonduine family compounds work via the concerted inhibition of both PARP-3 and PARP-16 together to trigger CFTR correction.

This raised an important point; we have previously shown that reduction in the amount of PARP-1 present has no effect on the ability of latonduine to correct CFTR (Carlile et al 2012). However, our group has also shown that ABT888 a specific PARP-1/2 inhibitor can produce some level of CFTR correction (Anjos et al 2012). Hence do these PARP inhibitors work through the same mechanism? To address this we tested

both MCG315 (1 μ M) and ABT888 (1 μ M) separately and together for their ability to correct F508del-CFTR in BHK cells in the HTS assay for 24 hours (Supplemental. Fig. 9A). The results show that in combination MCG315 and ABT888 work additively together suggesting a different method of action. To determine if ABT888 corrector function is mediated via PARPs-3 and 16 we used siRNA to PARP-16 and PARP-3 separately and together to knockdown expression and test whether less ABT888 was needed for CFTR correction (Supplemental. Fig. 9B, 9C and 5B). The results show that neither the knockdown of PARP-3 or parp-16 had any effect on the amount of ABT888 required for CFTR correction. Indeed when both PARPs were knocked down together ABT888 proved to be additive to the level of correction (Supplemental. Fig. 9C) providing strong evidence that the latonduine family of compounds and ABT888 correct CFTR by different mechanisms.

Addition of MCG315 blocks the PARP-16 mediated ribosylation of the unfolded protein response (UPR) sensor IRE-1.

We chose at this stage to focus on understanding the role of PARP-16 inhibition in the mechanism of action of latonduine family correction. Recent reports have shown that PARP-16 is a tail-anchored protein that is located at the ER membrane that can ribosylate the key UPR sensor IRE-1 and trigger the activation of the unfolded protein response through an increase in IRE-1 enzymatic activity. Moreover, the c-terminal ER luminal domain of PARP-16 transduces stress signals to its catalytic domain in the cytoplasm to regulate the ribosylation (Jwa and Chang, 2012). To determine what effect MCG315 would have on this molecular mechanism we tested the ability of PARP-

16 to ribosylate human IRE-1 α , (Fig.5A). Recombinant purified human IRE-1 α was incubated in the presence of recombinant PARP-16 and the level of isolated IRE-1 ribosylation was monitored using biotinylated NAD and a streptavidin conjugated HRP. The results show that PARP-16 ribosylates IRE-1 and this is almost abolished by latonduine. VX-809 a relatively potent CFTR corrector was unable to inhibit the ribosylation showing that this is not a general feature of CFTR correctors. Comparison with PARP-4 indicates that the ability to ribosylate IRE-1 was not a general feature of all PARPs. Furthermore, the effects of ABT888, (Fig.5B Supplemental. Fig 6A) indicated that the ability to inhibit PARP-16 was specific to the latonduine family compounds and this result was confirmed by radioactively labeling with ^{32}P –NAD. This was further confirmed by an experiment in which the PARP-16s ability to ^{32}P ribosylate IRE-1 signal could be competed away with increasing amounts of MCG315 with an EC_{50} of 4.778nM (Supplemental. Fig. 6B & 6C).

Latonduine blocks the ribosylation-dependent increase in IRE-1 activity.

Research has shown that ribosylation of IRE-1 is required for its activation during the UPR (Jwa and Chang, 2012). To test if the addition of MCG315 by inhibiting PARP-16 prevented IRE-1 activation we assayed both its RNase activity (Fig. 5C) and its kinase activities (Fig. 5D). In both instances the presence of MCG315 abrogated the increase in IRE-1 activity observed in the presence of PARP-16. Also on both occasions VX-809 did not prevent the increase in PARP-16 mediated IRE-1 activity. These results strongly suggest latonduine and its analogues function as CFTR correctors by preventing activation of UPR in cells through inhibition of PARP-16-mediated ribosylation of IRE-1 a key step during activation of the UPR.

To demonstrate that latonduine family members can block IRE-1 ribosylation *in vivo* we decided to immunoprecipitate IRE-1 from cells that had previously been treated with tunicamycin in the presence and absence of MCG315. We monitored the level of ribosylation on the IRE-1 by using a PAN-ADP-ribose binding agent (Millipore) (Supplemental. Fig. 7A & 7B). The results show that stimulation of the UPR triggers the appearance of ribosylated IRE-1 and that this was significantly reduced in the presence of MCG315. The signal detected was confirmed to be ribosylation as it was removable with incubation with O-acetyl-ADP-ribose deacetylase (MacroD1&2 [MyBioSource]) for 2 hours at 37°C. This strongly suggests that MCG315 is inhibiting PARP-16s ability to ribosylate IRE-1 *in-vivo*.

IRE-1 activity is required for latonduine mediated CFTR correction

To investigate if a reduction in IRE-1 expression increases latonduine-mediated correction. HEK cells expressing F508del-CFTR-3HA were treated with siRNA against IRE-1, incubated for 24 hours and then treated for a further 24 hours with latonduine (Fig. 6A) and MCG315 (Supplemental. Fig 7C). They were then tested for CFTR correction using the HTS assay. Surprisingly the results show that lowering IRE-1 expression reduced the potency of latonduine (and MCG315) as a corrector over a broad range of concentrations (10nM to 10µM) (The IRE-1 mRNA was reduced 84% as monitored by rtPCR, Supplemental. Fig 5C). This suggests that the presence of IRE-1 is required for correction by latonduine and its analogues.

To confirm this finding we repeated the reduction in IRE-1 expression by si-RNA to IRE-1 and monitored the effects of latonduine treatment on the maturation of F508-del-CFTR in HEK cells (Fig.6B). The results show that with latonduine treatment a

mature band C form of F508del-CFTR can be detected at three concentrations (100nM, 1 μ M and 10 μ M). However, upon the prior treatment with si-RNA to IRE-1 latonduine is unable to correct F508-del-CFTR at any of the concentrations tested (Fig.6B).

To determine if simply inhibiting IRE-1 activity would augment the CFTR by latonduine or MCG315 we tested the IRE-1 specific inhibitor 4 μ 8C (Zhang et al., 2014)(Fig. 6C) using the HTS assay. Interestingly 4 μ 8C treatment inhibits both latonduine and MCG315 mediated correction but it has no effect on VX-809 triggered CFTR correction. Hence correction by latonduine and its analogues requires not only the presence of IRE-1 but also some basal level of IRE-1 activity below that needed for the full UPR.

Latonduine does not effect the trafficking of other wild-type membrane bound glycoproteins.

Previous work has shown that latonduine as a proteostatic modulator can work on other mis-folded proteins from other trafficking diseases (Sampson et al. 2013). This raised the question of the effect of latonduine family members on other wild-type surface proteins To test its effect on other cell surface glycoproteins we monitored the level of CD44 in the plasma membrane upon latonduine and MCG315 (1 μ M) treatment for 24 hours (Supplemental. Fig 8A). CD44 is a cell surface protein involved to cell-cell interactions it is also a hyaluronic acid receptor and is known to be expressed in a broad spectrum of mammalian cells types including BHK (Tsukita et al 1994). We found that unlike CFTR the level of surface CD44 was not changed upon treatment. Further we undertook a series of western blots to monitor the levels of selected protein markers involved in protein trafficking and none of the ones tested showed any change upon either latonduine

MOL #102418

of MCG315 treatment (Supplemental. Fig. 8B). Together the data suggests that latonduine family members do not affect wild-type proteins.

DISCUSSION

Proteostasis modulator molecules that alter the homeostatic equilibrium of the cell can induce CFTR correction and are thus a promising therapeutic approach for cystic fibrosis. However, their targets and mechanisms of action have been elusive which hinders their development as lead compounds as rational SAR campaigns usually require the target of action and information on its structure.

We began this project with the corrector latonduine, a compound we had previously identified that gave a modest short circuit current response in polarized CFBE41o- cells expressing F508del CFTR ($0.66\mu\text{A}\cdot\text{cm}^{-3}$) (Carlile et al., 2012). Nevertheless, latonduine had the unique advantage for further optimization over other weak correctors in that we identified its likely target a member of the PARP family. Hence, the aims of this study were to identify an analogue of latonduine with improved CFTR corrector potency, to determine which members of the PARP family, when inhibited cause F508del-CFTR correction and to understand mechanistically how PARP inhibition leads to correction.

We prepared a small set of radical analogues of latonduine to rapidly determine which motifs are most critical for CFTR correction. We investigated removal of the aminopyrimidine ring and modifications on the pyrrole ring (MCG170, MCG172, MCG559, MCG980), however both MCG170 and MCG980 did not correct, nor were they better inhibitors of PARP-3 or PARP-16. However MCG172 and MCG559, which were synthesized by substitution of the bromine atom with a methyl group, both inhibited of PARP-3 and PARP-16. MCG559 was a slightly more potent inhibitor of PARP1 compared to MCG172, but both compounds gave F508del-CFTR correction.

Azepine ring side group alterations (MCG171 and MCG240) led to MCG240, an inhibitor of PARPs 1,3 and 16 that was most potent against PARP-3. MCG240 was also a corrector of F508del-CFTR trafficking.

Replacing the pyrrole ring with a phenyl ring led to MCG315 a stronger inhibitor of PARPs 1, 3 and 16 and more potent CFTR corrector. With a correction response in CFBE cells expressing F508del-CFTR that was 3.2% that of wild-type CFTR, MCG315 is almost 10-fold more potent than the parent molecule latonduine. Although MCG315 gave only 35% of the response obtained with VX-809 under the same conditions, which is more potent than many other CFTR correctors (Anjos et al., 2012; Carlile et al., 2007; Robert et al., 2008; Sampson et al., 2013; Zhang et al., 2012) When this is considered in combination with the fact the 10-fold increase in corrector potency was found after studying only 7 new analogues this suggests that the latonduine scaffold and its chemical space should be further explored. Moreover, MCG315 is a proteostasis modulator thus more likely to work for other protein trafficking diseases than would a pharmacological chaperone. This is supported by previous work in which latonduine was found to correct trafficking mutations from other trafficking diseases in particular the sulfonyl urea receptor mutation A116P (Sampson et al. 2013). This in turn suggests commonalities of mechanism in the retention of different misfolded proteins in the ER, which may be overcome by proteostatic modulators. This is intriguing when considered in combination to our findings regarding CD44. Hence it appears that mis-folded mutant proteins such as CFTR and SUR may be corrected by members of the latonduine family, however, wild-type surface glycoproteins and internal proteins involved in protein trafficking are not.

To understand the role of PARP inhibition in the mechanism of action of latonduine analogue mediated correction we first tested the most potent analogue (MCG315) against a panel of PARPs. We found that MCG315 is a potent inhibitor of two PARPs that is PARPs-3 & 16. In a previous paper we had reported on the role of PARP-3 in the mechanism of latonduine mediated correction of F508del-CFTR (Carlile et al. 2012). Upon testing with siRNA we discovered that not only was PARP-16 also involved in the mechanism of latonduine mediated CFTR correction but that when knocked down together with PARP-3 they acted in synergy and facilitated a certain level of correction even in the absence of MCG315. The level of correction did increase upon addition of MCG315 but only to the same level as MCG315 on its own with an EC_{50} 2nM. Given that the level of knockdown for both PARP mRNAs was approximately it is possible that 100% knockdown correct to the same level as MCG315 and that MCG315 CFTR corrector function is by the concerted inhibition of both PARP-3 and PARP-16 together.

We chose at this stage to explore MCG315s PARP-16 mediated CFTR corrector mechanism in greater detail. This approach was suggested by the finding that inhibition of PARP-16 was strongly correlated with correction of F508del-CFTR. Intriguingly PARP-16 is a tail-anchored protein that is located at the ER membrane and catalyzes mono-ADP ribosylation during the unfolded protein response (UPR) through activation of the stress sensors IRE-1 and PERK (Jwa and Chang, 2012). Moreover, the c-terminal ER luminal domain transduces stress signals to the PARP catalytic domain in the cytoplasm.

It is the modulation of this pathway that appears to be the mechanism of action of latonduine and its analogues that regulate F508del-CFTR trafficking. Latonduine action

requires the presence of IRE-1 and a basal level of IRE-1 enzymatic activity, but does not require full IRE-1 activation of the UPR to cause correction. Latonduine may exert its effect by blocking activation of the UPR through inhibition of PARP-16 possibly when there is some accumulation of misfolded CFTR. It is unclear at this stage why blocking this activity would increase F508del CFTR trafficking, however, it may be that inhibiting the UPR prevents the increased expression of chaperones such as calnexin and calreticulin which help process the mis-folded CFTR in the ER prior to transport for proteasomal degradation. Therefore allowing partially misfolded F508del-CFTR to escape the ER quality control (ERQC) and traffic to the plasma membrane. This work is in line with previous research that showed that inhibition of IRE-1 expression by the use of RNA interference will suppress correction of F508del-CFTR (Trzcinski-Daneluti AM, 2015) and also that some level of IRE-1 expression in cells is necessary for normal protein metabolism (Henis-Korenbilt, 2013).

MCG315 corrected F508del-CFTR trafficking in all assays tested however with considerable variation between the assays (from 35.4±2.1 % of wild type in BHK cells, to 3.2% in polarized CFBE cells). The reason for this 10-fold variation remains uncertain. It may be related to differences in the model species used (hamster vs. human cells), higher CFTR expression in BHK cells, or greater polarization of the CFBE cells (Ostedgaard et al., 2007). The present results suggest that the species-dependent cellular context and/or expression level may play a role. Similar variation in different cell types was reported after Aha1 knock down, which increased F508del-CFTR maturation in HEK293 but not CFBE cells (Wang et al., 2006). However, given the results in this paper it seems entirely possible that the differences in CFTR correction may be due at

least in part to differences in PARP-16, IRE-1 or PERK expression. Further it could be differences in the relative potency of the UPR to upregulate calnexin and calretulin in these various cell types play a role in the variable response.

The level of CFTR rescue needed for clinical benefit is unclear, with estimates up to 25% of wild-type function (Farmen et al., 2005; Zhang et al., 2009). Correction by MCG315 correction is less than by VX-809 but nevertheless compares favorably with other reported correctors (Van Goor et al., 2011). While MCG315 alone may not cause sufficient correction on its own, its combination with other correctors may yield therapeutic levels of F508del-CFTR rescue (Okiyoneda et al., 2013).

In conclusion the present work confirms the utility of the latonduine compound family as proteostatic modulators that correct F508del-CFTR. In particular with MCG315 that shows a dramatic 10-fold increase in corrector efficiency compared to latonduine. We show that latonduine appears to work via the concerted inhibition of both PARP-3 and PARP-16 together. Upon focusing on PARP-16, we provide evidence for its site of action in the NAD binding pocket of PARP-16. We demonstrate the mechanism of action for CFTR correction by latonduine through its role in PARP-16 inhibition and modulation of IRE-1 activity in this correction. The structure activity relationship and modeling studies suggest pyrrole ring replacement with a simpler ring such as in MCG315 promote binding in the NAD pocket of PARP-16. Such insights we believe will prove crucial in future rational structure based drug design. Together these results also open new areas of investigation; for example the role of IRE-1 modulation in CFTR rescue and provides a new tool for further studies of ER quality control in CF and other protein trafficking diseases.

ACKNOWLEDGEMENTS

AUTHORS CONTRIBUTIONS

1. *Participated in research design:* Carlile, Robert, Thomas, Hanrahan, Solari Anderson, Birault.
2. *Conducted experiments:* Carlile, Mattes, Yang, Hatley, Edge.
3. *Contributed new reagents or analytical tools:* Hatley, Birault.
4. *Performed data analysis:* Carlile, Robert, Solari, Edge, Hanrahan, Thomas, Birault.
5. *Wrote or contributed to the writing of the manuscript:* Carlile, Edge, Hatley Hanrahan, Thomas, Birault.

REFERENCES

Anjos, S.M., Robert, R., Waller, D., Zhang, D.L., Balghi, H., Sampson, H.M., Ciciriello, F., Lesimple, P., Carlile, G.W., Goepf, J., *et al.* (2012). Decreasing Poly(ADP-Ribose) Polymerase Activity Restores DeltaF508 CFTR Trafficking. *Front Pharmacol* 3, 165.

Bebok Z, C.J., Wakefield J, Parker W, Li Y, Varga K, (2005). Failure of cAMP agonists to activate rescued deltaF508 CFTR in CFBE41o- airway epithelial monolayers. *Journal of Physiology Dec 1 569(Pt2)* 601-615.

Berman, H.M., Westbrook, J., Feng, Z., Gilliland, G., Bhat, T.N., Weissig, H., Shindyalov, I.N., and Bourne, P.E. (2000). The Protein Data Bank. *Nucleic Acids Res* 28, 235-242.

Carlile, G.W., Keyzers, R.A., Teske, K.A., Robert, R., Williams, D.E., Linington, R.G., Gray, C.A., Centko, R.M., Yan, L., Anjos, S.M., *et al.* (2012). Correction of F508del-CFTR trafficking by the sponge alkaloid latonduine is modulated by interaction with PARP. *Chem Biol* 19, 1288-1299.

Carlile, G.W., Robert, R., Zhang, D., Teske, K.A., Luo, Y., Hanrahan, J.W., and Thomas, D.Y. (2007). Correctors of protein trafficking defects identified by a novel high-throughput screening assay. *Chembiochem* 8, 1012-1020.

Cheng, S.H., Gregory, R.J., Marshall, J., Paul, S., Souza, D.W., White, G.A., O'Riordan, C.R., and Smith, A.E. (1990). Defective intracellular transport and processing of CFTR is the molecular basis of most cystic fibrosis. *Cell* 63, 827-834.

Clancy, J.P., Rowe, S.M., Accurso, F.J., Aitken, M.L., Amin, R.S., Ashlock, M.A., Ballmann, M., Boyle, M.P., Bronsveld, I., Campbell, P.W., *et al.* (2012). Results of a phase IIa study of VX-809, an investigational CFTR corrector compound, in subjects with cystic fibrosis homozygous for the F508del-CFTR mutation. *Thorax* 67, 12-18.

Egan, M.E., Pearson, M., Weiner, S.A., Rajendran, V., Rubin, D., Glockner-Pagel, J., Canny, S., Du, K., Lukacs, G.L., and Caplan, M.J. (2004). Curcumin, a major constituent of turmeric, corrects cystic fibrosis defects. *Science* 304, 600-602.

Farmen, S.L., Karp, P.H., Ng, P., Palmer, D.J., Koehler, D.R., Hu, J., Beaudet, A.L., Zabner, J., and Welsh, M.J. (2005). Gene transfer of CFTR to airway epithelia: low levels of expression are sufficient to correct Cl⁻ transport and overexpression can generate basolateral CFTR. *Am J Physiol Lung Cell Mol Physiol* 289, L1123-1130.

Henis-Korenbilt, M.S.S.B.-H.C.k.a.S. (2013). The IRE-1 ER stress-response pathway is required for normal secretory -protein metabolism in *C. elegans*. *Journal of cell science* 126((18)), 4136-4146.

Hwang, T.C., and Sheppard, D.N. (2009). Gating of the CFTR Cl⁻ channel by ATP-driven nucleotide-binding domain dimerisation. *J Physiol* 587, 2151-2161.

Jwa, M., and Chang, P. (2012). PARP16 is a tail-anchored endoplasmic reticulum protein required for the PERK- and IRE1alpha-mediated unfolded protein response. *Nat Cell Biol* 14, 1223-1230.

Lehtio, L., Jemth, A.S., Collins, R., Loseva, O., Johansson, A., Markova, N., Hammarstrom, M., Flores, A., Holmberg-Schiavone, L., Weigelt, J., *et al.* (2009). Structural basis for inhibitor specificity in human poly(ADP-ribose) polymerase-3. *J Med Chem* 52, 3108-3111.

Lukacs, G.L., Chang, X.B., Bear, C., Kartner, N., Mohamed, A., Riordan, J.R., and Grinstein, S. (1993). The delta F508 mutation decreases the stability of cystic fibrosis transmembrane conductance regulator in the plasma membrane. Determination of functional half-lives on transfected cells. *J Biol Chem* 268, 21592-21598.

Ma, T., Thiagarajah, J.R., Yang, H., Sonawane, N.D., Folli, C., Galietta, L.J., and Verkman, A.S. (2002). Thiazolidinone CFTR inhibitor identified by high-throughput screening blocks cholera toxin-induced intestinal fluid secretion. *J Clin Invest* 110, 1651-1658.

Mhlanga, P., Wan Hassan, W.A., Hamerton, I., and Howlin, B.J. (2013). Using combined computational techniques to predict the glass transition temperatures of aromatic polybenzoxazines. *PLoS One* 8, e53367.

Okiyoneda, T., Veit, G., Dekkers, J.F., Bagdany, M., Soya, N., Xu, H., Roldan, A., Verkman, A.S., Kurth, M., Simon, A., *et al.* (2013). Mechanism-based corrector combination restores DeltaF508-CFTR folding and function. *Nat Chem Biol* 9, 444-454.

Ostedgaard, L.S., Rogers, C.S., Dong, Q., Randak, C.O., Vermeer, D.W., Rokhlina, T., Karp, P.H., and Welsh, M.J. (2007). Processing and function of CFTR-DeltaF508 are species-dependent. *Proc Natl Acad Sci U S A* 104, 15370-15375.

Rasband, W.S. (2011). ImageJ (<http://imagej.nih.gov/ij/1997-2011>: National Institutes of Health, Bethesda, Maryland USA), pp.

Riordan, J.R., Rommens, J.M., Kerem, B., Alon, N., Rozmahel, R., Grzelczak, Z., Zielenski, J., Lok, S., Plavsic, N., Chou, J.L., *et al.* (1989). Identification of the cystic fibrosis gene: cloning and characterization of complementary DNA. *Science* 245, 1066-1073.

Robert, R., Carlile, G.W., Liao, J., Balghi, H., Lesimple, P., Liu, N., Kus, B., Rotin, D., Wilke, M., de Jonge, H.R., *et al.* (2010). Correction of the Delta phe508 cystic fibrosis transmembrane conductance regulator trafficking defect by the bioavailable compound glafenine. *Mol Pharmacol* 77, 922-930.

Robert, R., Carlile, G.W., Pavel, C., Liu, N., Anjos, S.M., Liao, J., Luo, Y., Zhang, D., Thomas, D.Y., and Hanrahan, J.W. (2008). Structural analog of sildenafil identified as a novel corrector of the F508del-CFTR trafficking defect. *Mol Pharmacol* 73, 478-489.

Rubenstein, R.C., Egan, M.E., and Zeitlin, P.L. (1997). In vitro pharmacologic restoration of CFTR-mediated chloride transport with sodium 4-phenylbutyrate in cystic fibrosis epithelial cells containing delta F508-CFTR. *J Clin Invest* 100, 2457-2465.

Sampson, H.M., Lam, H., Chen, P.C., Zhang, D., Mottillo, C., Mirza, M., Qasim, K., Shrier, A., Shyng, S.L., Hanrahan, J.W., *et al.* (2013). Compounds that correct F508del-CFTR trafficking can also correct other protein trafficking diseases: an in vitro study using cell lines. *Orphanet J Rare Dis* 8, 11.

Sato, S., Ward, C.L., Krouse, M.E., Wine, J.J., and Kopito, R.R. (1996). Glycerol reverses the misfolding phenotype of the most common cystic fibrosis mutation. *J Biol Chem* 271, 635-638.

Trzcinski-Daneluti AM, C.A., Nguyen L, Murchie R, Jiang C, Moffat J, Pelletier L, Rotin D. (2015). RNA Interference Screen to Identify Kinases That Suppress Rescue of F508del-CFTR. *Molecular & cellular proteomics : MCP Jun; 14(6)*, 1569-1583.

Van Goor, F., Hadida, S., Grootenhuis, P.D., Burton, B., Stack, J.H., Straley, K.S., Decker, C.J., Miller, M., McCartney, J., Olson, E.R., *et al.* (2011). Correction of the F508del-CFTR protein processing defect in vitro by the investigational drug VX-809. *Proc Natl Acad Sci U S A* 108, 18843-18848.

Wang, X., Venable, J., LaPointe, P., Hutt, D.M., Koulov, A.V., Coppinger, J., Gurkan, C., Kellner, W., Matteson, J., Plutner, H., *et al.* (2006). Hsp90 cochaperone Aha1 downregulation rescues misfolding of CFTR in cystic fibrosis. *Cell* 127, 803-815.

Zhang, D., Ciciriello, F., Anjos, S.M., Carissimo, A., Liao, J., Carlile, G.W., Balghi, H., Robert, R., Luini, A., Hanrahan, J.W., *et al.* (2012). Ouabain Mimics Low Temperature Rescue of F508del-CFTR in Cystic Fibrosis Epithelial Cells. *Front Pharmacol* 3, 176.

Zhang, L., Button, B., Gabriel, S.E., Burkett, S., Yan, Y., Skiadopoulos, M.H., Dang, Y.L., Vogel, L.N., McKay, T., Mengos, A., *et al.* (2009). CFTR delivery to 25% of surface epithelial cells restores normal rates of mucus transport to human cystic fibrosis airway epithelium. *PLoS Biol* 7, e1000155.

Zhang, L., Nosak, C., Sollazzo, P., Odisho, T., and Volchuk, A. (2014). IRE1 inhibition perturbs the unfolded protein response in a pancreatic beta-cell line expressing mutant proinsulin, but does not sensitize the cells to apoptosis. *BMC Cell Biol* 15, 29.

MOL #102418

Footnotes

We thank the Canadian Institutes of Health Research for their support [CIHR-216385 and CIHR-218654].

LEGENDS FOR FIGURES

Figure 1. Latonduine analogues correct F508del-CFTR localization. (A) The structures of latonduine and its analogues. (B) Baby hamster kidney (BHK) cells expressing F508del-CFTR tagged with three hemagglutinin motifs (3HA) were exposed to latonduine analogues (10 μ M) for 24 hours and then tested using the HTS assay for changes in surface CFTR expression. (C) Immunoblot of BHK cells expressing F508del-CFTR, which were treated with 10 μ M latonduine and analogues for 48h and probed for CFTR expression using mouse anti-CFTR antibody. Band C corresponds to the mature, complex-glycosylated form of CFTR and band B to the immature core-glycosylated, ER associated protein. Tubulin was probed as a protein loading control. BHK cells expressing wild-type CFTR (WT) used as a control. (D) Densitometry of the immunoblot in C normalized using the tubulin signal for protein loading. The bars indicate the percentage of total CFTR in each glycoform (band B or C). The data indicate means \pm SEM. Each experiment was completed in triplicate.

Figure 2. Latonduine analogues act as correctors of CFTR function. The latonduine analogue mediated rescue of F508del-CFTR function in human bronchial epithelial cells (CFBE41o $^+$). The basolateral membrane was permeabilized using nystatin and an apical-to-basolateral chloride gradient was imposed, consequently CFTR-mediated current are shown as positive. (A) Bar graph showing the stimulation of short-circuit current (ΔI_{sc}) induced by acute addition of forskolin + genistein, defined as the difference between the sustained phase of the current response after genistein and the baseline immediately

MOL #102418

before stimulation. (B) Representative I_{sc} responses to 10 μ M forskolin, 50 μ M genistein and 10 μ M CFTRinh-172 after 24 hour exposure of F508del-CFTR CFBE cells to 0.1% DMSO (vehicle), 10 μ M MCG315 (315), or low temperature (LT) (29°C). C. Concentration series for correction by latonduine and MCG315 after incubation for 24 h measured BHK cells using the HTS assay. (D) Time course of the corrector response to latonduine and MCG315 tested at 10 μ M.

Figure 3. Latonduine interacts with PARP-16 and inhibits PARP enzymatic activity.

(A) A 1 μ g sample of purified, recombinant human PARP-16, (PARP 16) was pre-cleared using beads that had been incubated with biotin. The PARP-16 was then incubated with beads that had been pre-incubated with biotin (BEADS) or with beads pre-loaded with biotinylated latonduine (B-L) and washed prior to SDS PAGE and staining with Coomassie blue. Similar pulldowns using biotinylated latonduine were undertaken in the presence of increasing concentrations of latonduine and MCG315 (0, 1nM, 10nM, 100nM 1 μ M). (B) The intensity of each band of PARP-16 in A was plotted. (C) The ability of latonduine analogues to inhibit recombinant human PARPs 1, 3 and 16 enzyme activities respectively, as measured using the HT Universal Chemiluminescent PARP Assay Kit (Trevigen MD). All compounds were tested at 10 μ M. Note the substrate used for PARP-16 was recombinant human IRE-1 a known PARP-16 target. The values given for each treatment are the percentage PARP activity obtained for that treatment when compared to a standardized control activity for each of the PARPs tested. The same amount of PARP activity against a reference substrate was used in each assay. VX-809

MOL #102418

and ABT888 are tested as controls (D) Similar to part C, The specificity of MCG315 (1 μ M) as a PARP inhibitor as measured using the HT Universal Chemiluminescent PARP Assay Kit (Trevigen MD) again using IRE-1 for PARP-16 and a range of PARP enzymes (PARPs-1, 2, 3, 4, 5a, 5b, 11 and 16).

Figure 4. PARP structures and modeling the position of latonduine and MCG315 and reducing PARP-16 expression augments MCG315 CFTR corrector activity (A)

Overlay of PARP-1 (cyan), PARP-3 (orange) and PARP-16 (green) with 3-aminobenzamide ligand (white), showing structurally similar C-terminal binding domains surrounding the ligand but a different N-terminal domain for PARP-16 which lacks the α -helix ‘roof’ of the nicotinamide pocket.

(B) The docking model for latonduine bound to PARP-3, showing the extra interactions made by the α -helix D284 and the D-loop G406. Latonduine is shown as a cyan, space-fill model. The backbone of the protein is shown as an orange ribbon and the neighboring amino acids as magenta stick models. G406 is at the top of the picture and D284 is at the top left (see white arrows). (C) MCG315 docking model in PARP-1 (orange) and (D) PARP-16 (green), showing change of enzyme surface to the right of the pictures, due to replacement of K903:E988 salt bridge in PARP-1 by leucine and tyrosine in PARP-16. The ADP molecule is shown in white. (E) The amide recognition pocket of PARP-1, PARP-3 and PARP-16, with the 3-aminobenzamide ligand of crystal structure 4F0D (PARP-16) is shown with the ADP shown in white. Hydrogen bonding is provided by the glycine amide backbone and, in the case of PARP-1 and PARP-3, a serine hydroxyl. Histidine and two tyrosines aromatic side chains lines the pocket. (F) Cell

MOL #102418

surface CFTR in HEK cells expressing F508del-CFTR, treated with different concentrations of MCG315 (0nM, 100pM, 1nM, 10nM, 100nM, 1μM, 10μM and 100μM) in combination with siRNA knockdown of control scrambled siRNA (black circle) or PARP-3 (black square) or PARP-16 (open square) or both PARPs-3 &16 (open triangle) for 24h prior to 24h incubation with MCG315.

Figure 5. PARP-16 ribosylates IRE-1, this ribosylation increases the activity of IRE-1, MCG315's inhibition of PARP-16 blocks ribosylation of IRE-1 and prevents the increase in its activity. (A) IRE-1 ribosylation was measured *in vitro* using the HT Universal Chemiluminescent PARP assay kit (Trevigen). The same amount of PARP-16 enzyme (0.5 Units) was used against a reference substrate in each assay. In the presence and absence of MCG315 (10μM), VX-809 (1μM). PARP-4 was used as a negative control. (B) Similar experiment to part A, except IRE-1 ribosylation was measured by incorporation of ³²P NAD and ABT888 (1μM) was used as a 'non PARP-16' PARP inhibitor. (C) Measurement of IRE-1 kinase activity using similar treatments to A (D) Measurement of IRE-1 RNAase activity using similar treatments to A.

FIGURE 6. Reduction of IRE-1 expression or inhibition in ire-1 function by 4μ8C inhibits latonduine mediated F508del-CFTR correction. (A) Cell surface CFTR in HEK293 cells expressing F508del-CFTR, treated with different concentrations of latonduine (0, 100pM, 1nM, 10nM, 100nM, 1μM, 10μM) in combination with siRNA knockdown of IRE-1 (white) or control siRNA (with scrambled sequence, black) for 24h and then incubated for a further 24 hours with latonduine. All results are shown as means of triplicate samples ± SEM. (B) Similar experiment to part A, except latonduine

MOL #102418

mediated correction was visualized via immunoblotting (C) Measurement of CFTR correction by HTS assay with latonduine (10 μ M) MCG315 (10 μ M) and VX-809 (1 μ M) in the presence and absence of 4 μ 8 \square (10 μ M). The numbers given for each treatment are the percentage of wild-type surface CFTR signal detected in the assay.

FIGURE 1

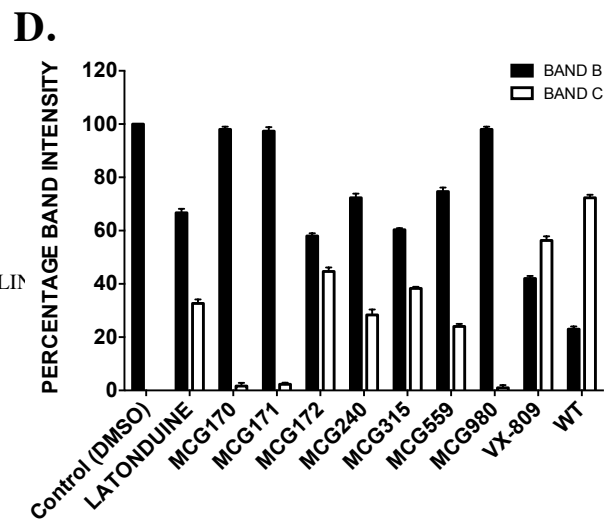
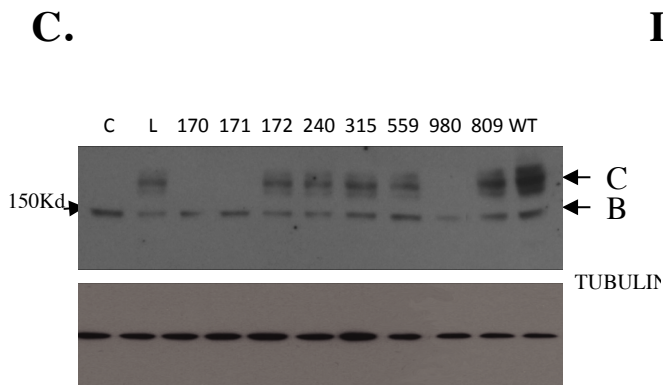
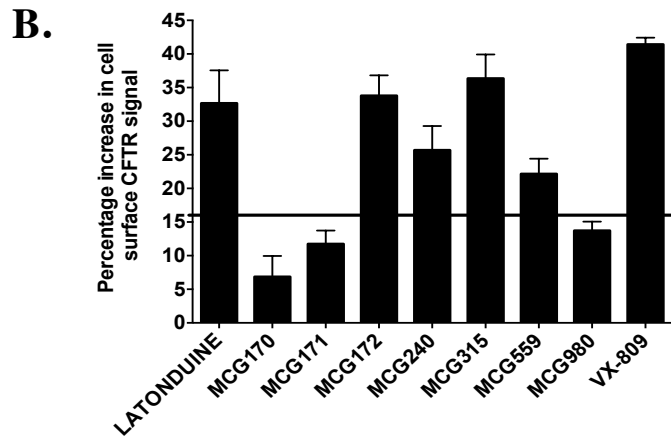
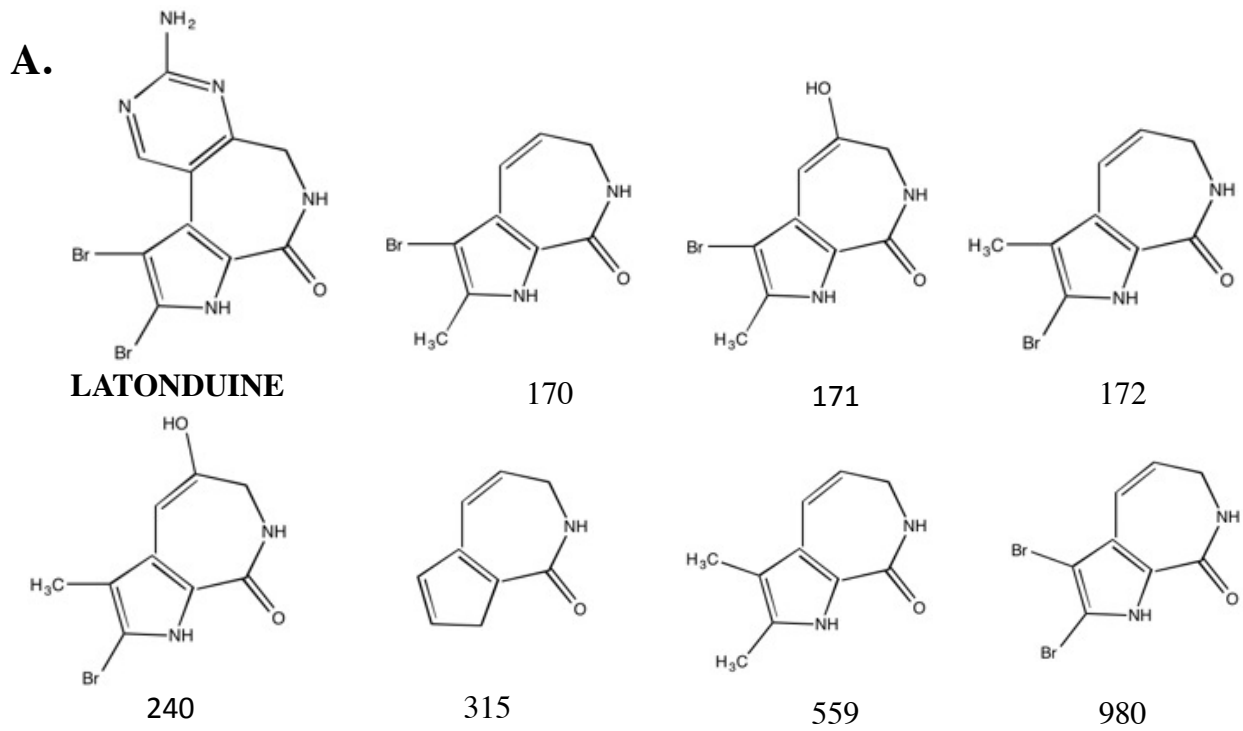


FIGURE 2

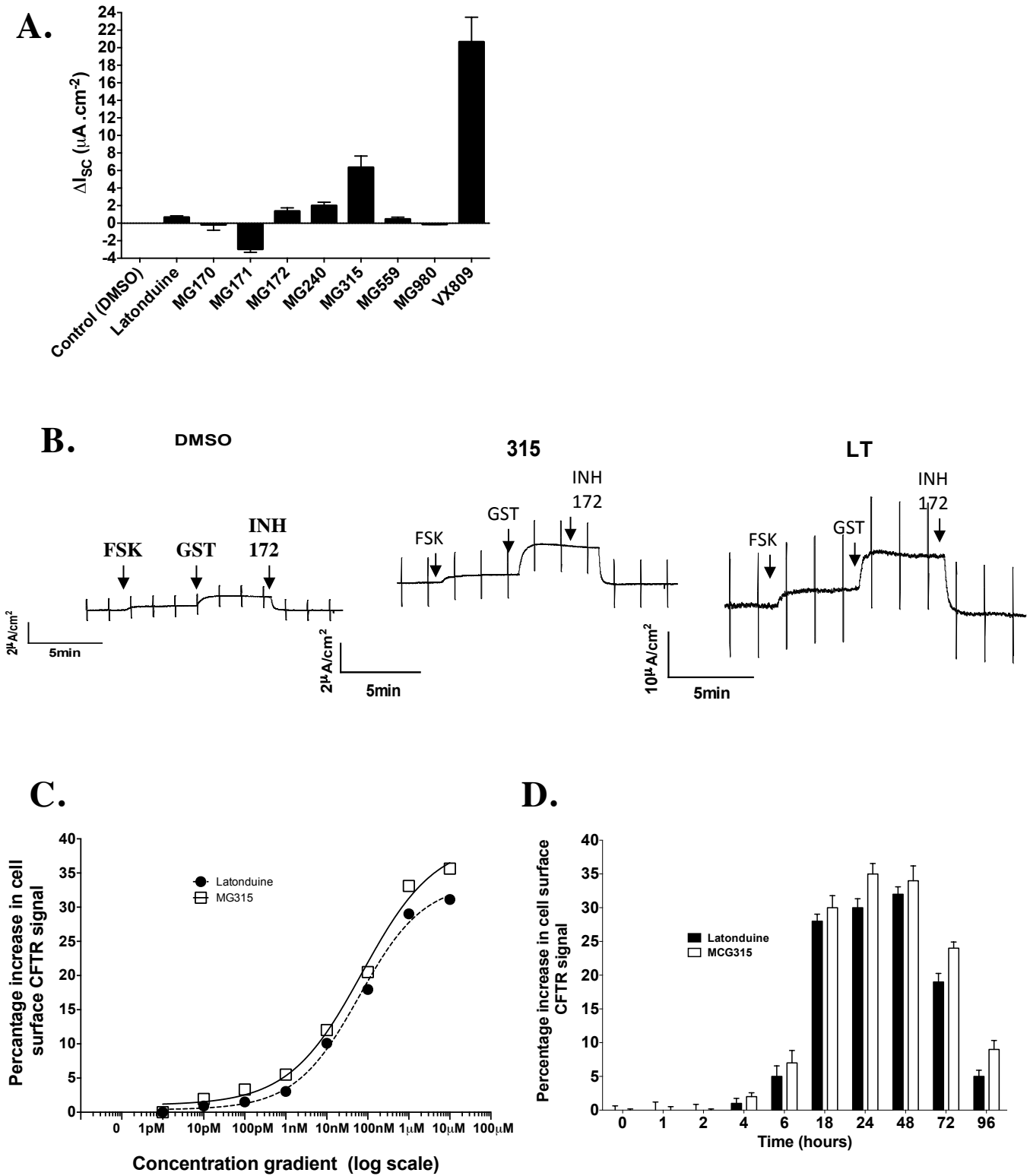
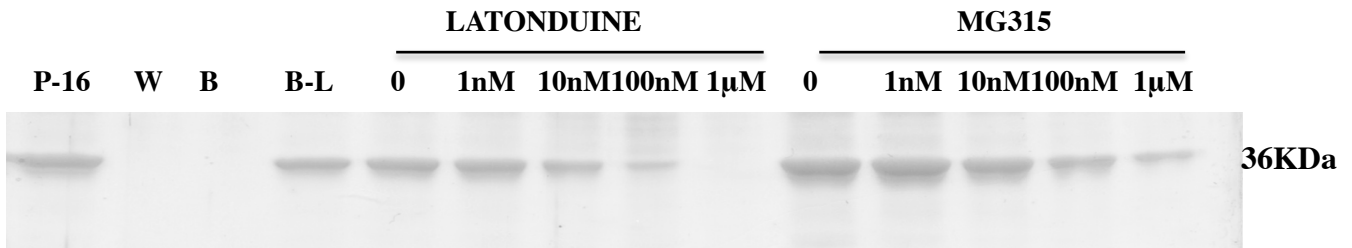
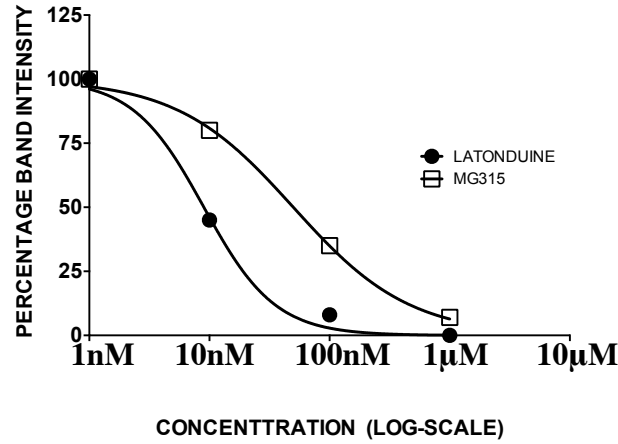


FIGURE 3

A.



B.



C.

	PARP-1	PARP-3	PARP-16	
Control	97.9	100.4	100.9	<div style="display: flex; align-items: center;"> <div style="width: 10px; height: 10px; background-color: red; margin-right: 5px;"></div> <div style="width: 10px; height: 10px; background-color: orange; margin-right: 5px;"></div> <div style="width: 10px; height: 10px; background-color: yellow; margin-right: 5px;"></div> <div style="width: 10px; height: 10px; background-color: lightblue; margin-right: 5px;"></div> <div style="width: 10px; height: 10px; background-color: blue; margin-right: 5px;"></div> <div style="margin-left: 10px;"> <p>HIGH</p> <p>INHIB</p> <p>LOW</p> <p>INHIB</p> </div> </div>
Lat 10µM	67.8	15.442	32.736	
MG170 10µM	91.1	46.651	51.874	
MG171 10µM	88.206	44.953	93.746	
MG172 10µM	39.427	33.573	24.577	
MG240 10µM	40.039	11.455	22.648	
MG315 10µM	31.671	19.703	5.039	
MG559 10µM	6.935	31.307	27.307	
MG980 10µM	43.985	64.331	99.962	
VX-809 10µM	98.3	94.7	101.3	
ABT888 10µM	0.924	89.7	95.9	

D.

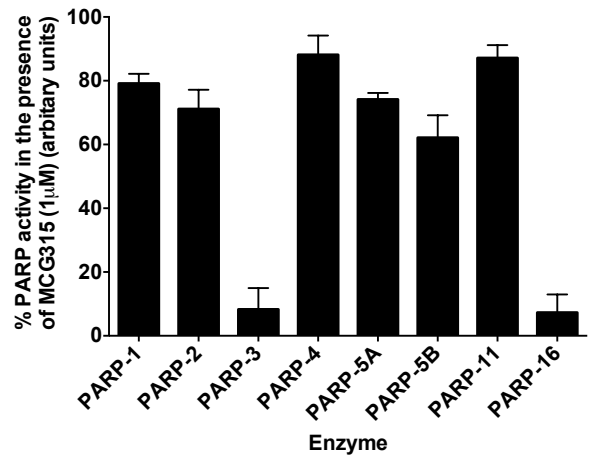


FIGURE 4

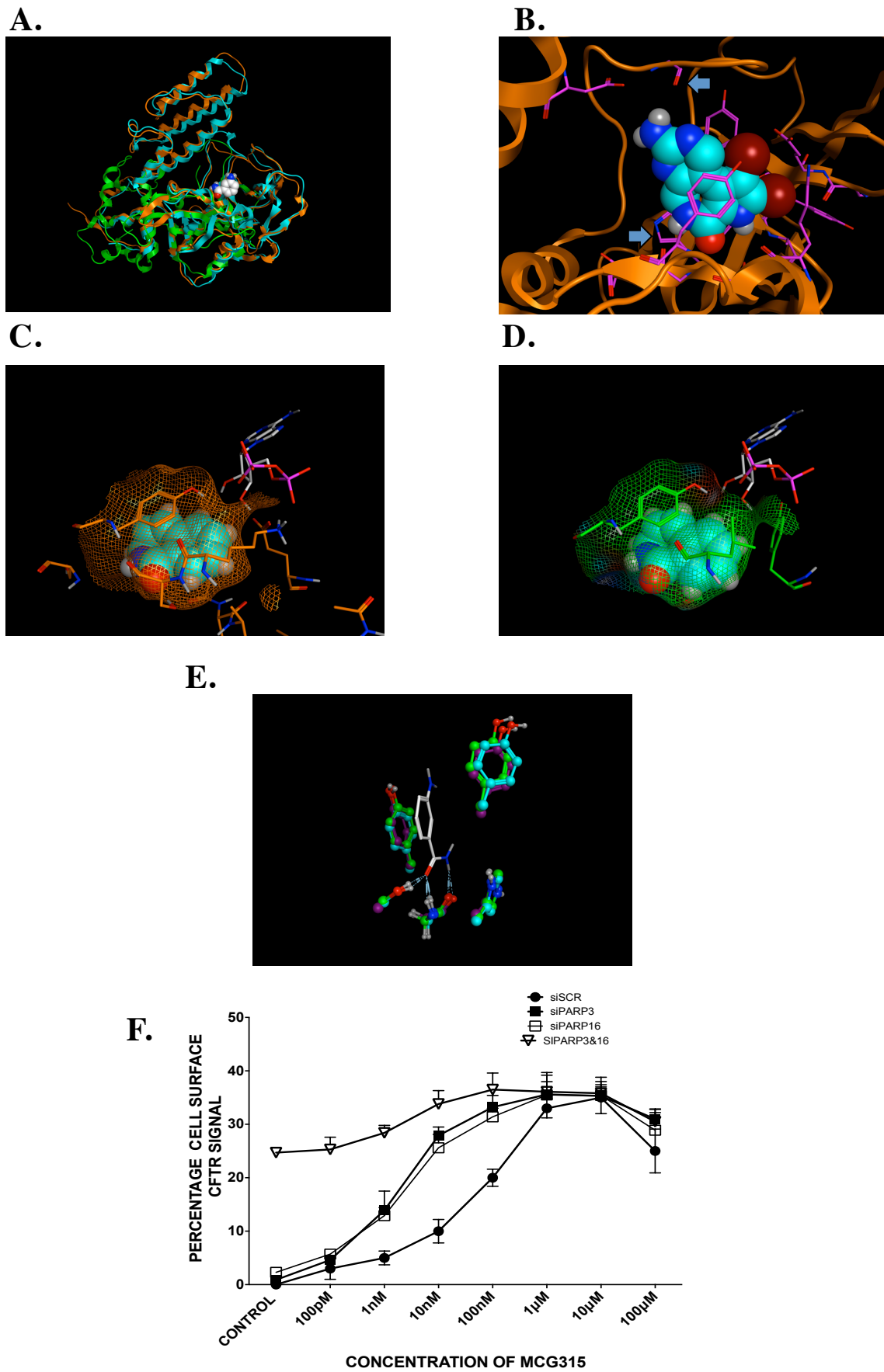
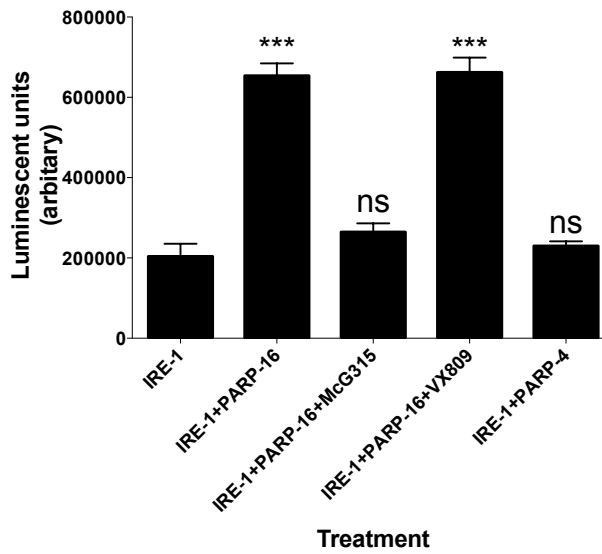
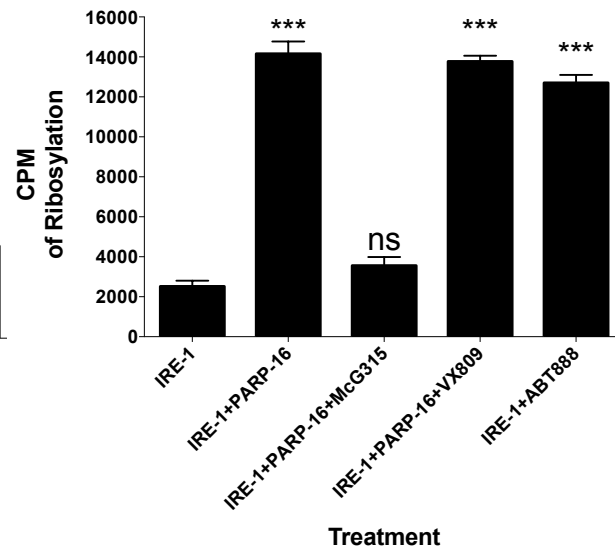


FIGURE 5

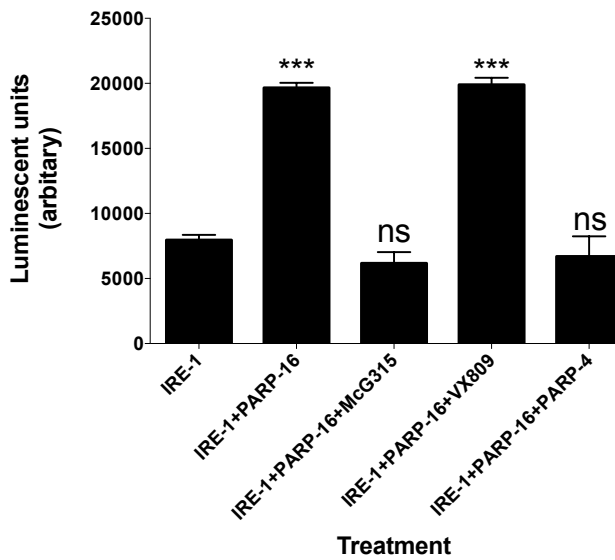
A.



B.



C.



D.

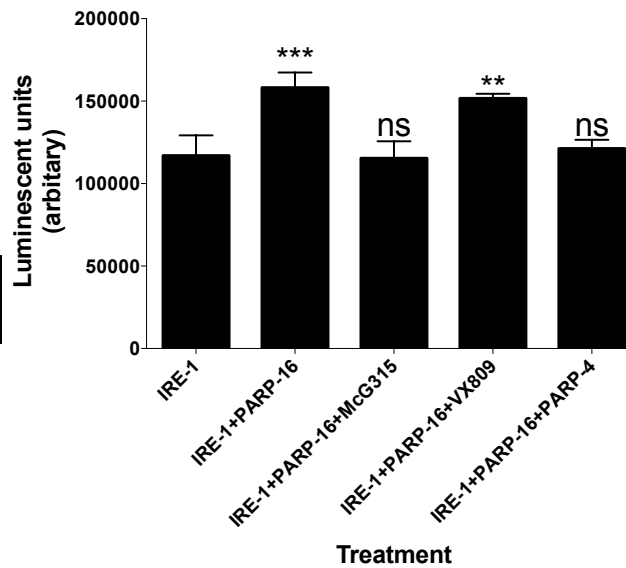
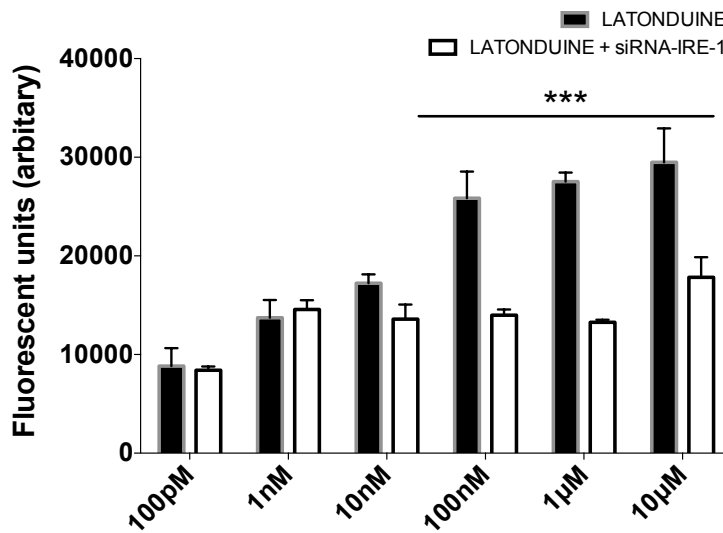
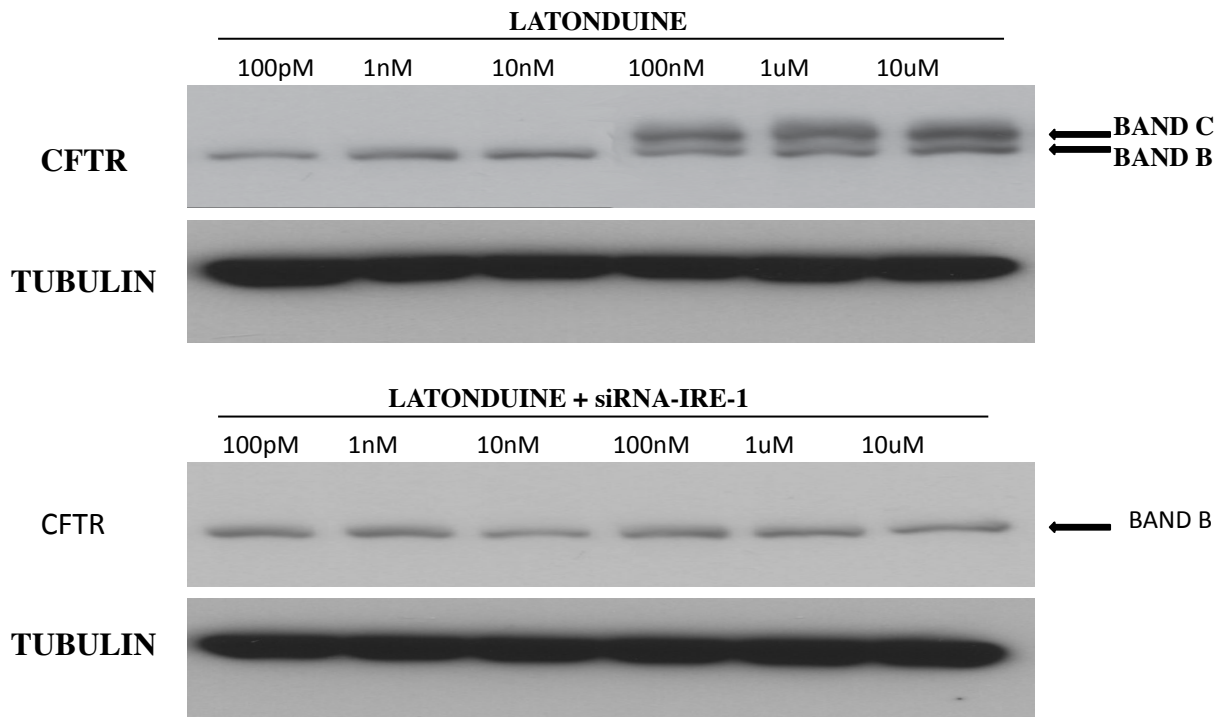


FIGURE 6

A.



B.



C.

	100pM	1nM	10nM	100nM	1uM	10uM	
LATONDUINE	8.2	9.6	10.4	11.2	14.6	10.5	
LATONDUINE+4U8C	2.1	3	5.2	8.5	7.6	8.5	
MCG315	9.1	11.2	12.1	13.2	17	13.9	
MCG315+4U8C	2.6	2.5	5.3	8.2	8.2	9.8	
VX809	10.1	10.6	12.9	17	17.9	12.1	
VX809+4U8C	10.5	11.5	13.4	15.4	16.9	12.9	